SHAPE SPLITTING FROM MEDIAL LINES USING THE 3-4 CHAMFER DISTANCE

Edouard Thiel ; Annick Montanvert

Laboratoire TIM3 - IMAG - Equipe RFMQ - USR B 00690
CERMO BP 53X - 38041 GRENOBLE Cedex - FRANCE

1. INTRODUCTION

Image analysis and shape description usually require to split the extracted objects into simpler components. This is mainly the case in the application field of cytology or material studies where some aggregations need to be separated into cells or seeds (see Fig. 1).

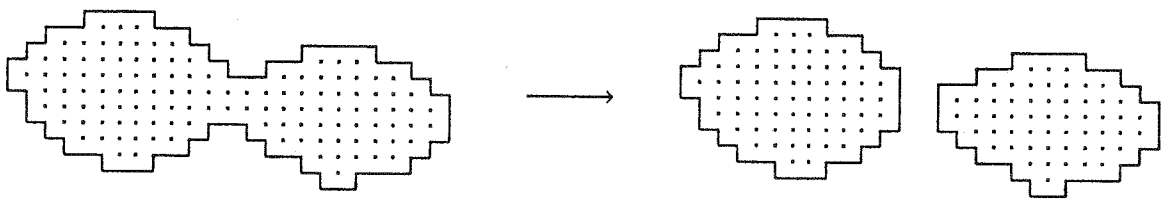

Fig.1. Decomposition of an object into simpler components.

Iterative methods based on mathematical morphology theory are usable, but the number of iterations depends on the width of the shape[1]. We are interested in internal representations of shape (as opposed to boundary representations) and in the development of methods which are width-independant, medial line representations allow to achieve this goal. They are built by sequential algorithms which require a constant number of image scannings.

Such a process is defined by the following stages :

- a distance transformed picture is computed from the binary input image,
- a medial line (weighted skeleton) is extracted from the distance transformed picture,
- characteristic points of narrow areas in the shape are isolated from the medial line,
- splitting arcs are drawn from these points to the shape boundary.

If the formulation is pretty clear, each of the stages is a problem in itself.

Such an approach was proposed based on the chessboard distance[2], but because of this distance in itself, the process is not invariant under rotation, and so a narrow area might not be detected depending on the orientation of the shape in the picture.

A better distance is required to improve the decomposition process, but all the next stages have to be adapted.

In this paper we propose a solution based on the 3-4 chamfer distance, which is a good

approximation of the euclidean distance and allows fast and robust algorithms. After a short presentation of the discrete distance transforms and of the medial axis for the 3-4 chamfer distance transform, we'll detail our connection process to get a medial line, how the characteristic points of narrowing are extracted and how the splitting process is performed. Finally some results are presented.

2. DISCRETE DISTANCE TRANSFORMS

From a binary image, the distance transformed picture is such that every point in an object is assigned to the value of its distance to the background. In the case of the square lattice, the basic distances are the City Block distance (d_4) and the Cheesboard distance (d_8) ; for two points P(i_P, j_P) et Q(i_Q, j_Q), d_4 and d_8 are defined by :

$$d_4(P, Q) = |i_P - i_Q| + |j_P - j_Q| \; ; \; d_8(P, Q) = \max(|i_P - i_Q| , |j_P - j_Q|)$$

Both parallel or sequential algorithms might be applied ; on a sequential computer, we do prefer a sequential process. Such an algorithm requires two scannings of the picture, a forward scanning followed by a backward scanning. Unfortunately, the values they provide on a distance transformed picture are far away from the euclidean values (41% of relative error for d_4 and 29% of relative error for d_8), and they depend on the orientation of the shape[3].

The euclidean distance is not that easy to compute using a fast sequential process, and the two pictures where the result is stored (horizontal and vertical values to the nearest background point) have to be manipulated[4,5].

Chamfer distances are very satistactory considering the speed constraint on a sequential computer, and the relative error compared to the euclidean distance. The result is stored in a matrix of integers, which is the usual representation of a picture[6].

They are based on the assignment of some weights to some elementary movings on the lattice, related to the true distance between the points. A chamfer distance is defined by a (2u+1 x 2v+1) kernel $m(h,k)$ (h=-u..u, k=-v..v) which is applied on the binary picture. (m (h,k) = ß) means that the distance from the point (i,j) to the point (i+h, j+k) is equal to m(h,k).

In fact only the first values depending on a new direction need to be defined on the kernel. Computing the distance transform picture from the kernel can be done using a parallel algorithm, but a main point is that it is equivalent to a sequential algorithm, needing a forward and a backward scanning, with two kernels which are deduced from the kernel m.

For example, for a 3x3 kernel, two values a and b appear. For the parallel algorithm, the kernel is m (see Fig. 2.a) ; for the sequential algorithm, m is splitted into two kernels $m_{forward}$ and $m_{backward}$ (see Fig. 2.b).

$$\begin{pmatrix} b & a & b \\ a & 0 & a \\ b & a & b \end{pmatrix} \qquad \begin{pmatrix} b & a & b \\ a & 0 & \end{pmatrix} \qquad \begin{pmatrix} & 0 & a \\ b & a & b \end{pmatrix}$$

a b c

Fig. 2. Kernels : m (a), $m_{forward}$ (b), $m_{backward}$ (c).

These kernels are used by the following algorithm on a matrix A in which the pixels are initially assigned to 0 for the background and to ∞ for the objects.

Forward scanning:

for i = 1 to N do for j = 1 to M do

A(i,j) = minimum $_{(h,k)}$ (A (i+h, j+k) + $m_{forward}$ (h,k)) ;

Backward scanning:

for i = N to 1 do for j = M to 1 do

A(i,j) = minimum $_{(h,k)}$ (A (i+h, j+k) + $m_{backward}$ (h,k)) ;

Using this formulation, d_4 is defined by a=1, b=∞, and d_8 is defined by a=b=1.

Other values assigned to the 3 x 3 kernel allow to reduce the error compared to the euclidean distance. The maximum relative error might be minimized inside the square including the picture and the values obtained for the kernel are approximated by integers[6]. The values a=3, b=4 are recommended, the maximum relative error is equal to 8.09%, instead of 4.49% for real values of a and b. The resulting disk is an octogon.

The size of the kernel can be increased, and the same optimization principle performed. For example, on a 5 x 5 kernel, the weigths are the following : $\begin{matrix} 7 & 11 \\ P & 5 \end{matrix}$ and the generated disks are 16 sides polygons (see Fig. 3). Using larger kernels, the quality of the distance compared to the euclidean distance can be improved ; but the computation time of the distance transform increases because the kernel is larger, and the distance values to store are larger.

Consequently, we choose the 3-4 chamfer distance to be able to solve the next stages of the splitting process. This choice is confirmed by the results we'll get.

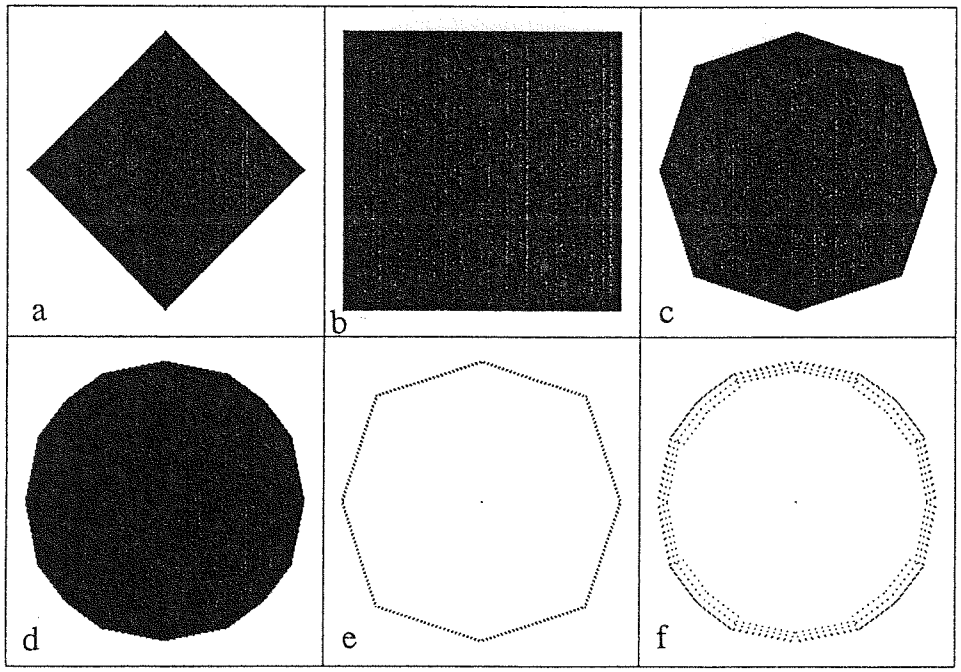

Fig.3. Disks for d_4 (a), d_8 (b), $d_{3\text{-}4}$ (c), $d_{5\text{-}7\text{-}11}$ (d) and pseudo local maxima in distance transformed pictures for $d_{3\text{-}4}$ (e), $d_{5\text{-}7\text{-}11}$ (f).

3. MEDIAL AXIS FOR THE 3-4 CHAMFER DISTANCE

One of the most important applications of distance transforms is to provide a shape representation method based on a covering of the shape by maximal disks fitting in it. A disk is said to be maximal if it is not completely included in any other disk (but it might be

included in the union of several other disks). The locus of the centers, completed by their radii, define the medial axis of the original picture. Medial axis is both useful for image coding and shape description[7].

Of course the process is reversible : from a medial axis picture, an inverse distance transform (using two scannings of the picture) can be applied to recover the initial shapes.

Using d_4 or d_8 distance, the medial axis points are easily extracted because they are large local maxima (in the 4-neighborhood for d_4 and in the 8-neighborhood for d_8) in the distance transformed picture.

An equivalent formulation is that their value cannot be computed substracting 1 to the value of any of their neighbors. If we adapt this formulation to a chamfer distance, we'll say that :

$$(x,y) \in \text{Medial Axis} \Leftrightarrow DT(x,y) > \text{Max}_{(h,k)} \{ DT(x+h,y+k) - m(h,k) \} \quad (1)$$

where DT denotes the matrix of the Distance Transformed picture.

Unfortunately, if this characterization is available for d_4 and d_8, it is not true for any chamfer distance. Indeed the points, which are extracted, are necessary to obtain the true distance values using the reverse distance transform, but they are not necessary to define the shape (because the points in the shape only need to be assigned to a non zero value by the inverse distance transform, at least this value must be one). These points are called pseudo local maxima (see Fig. 3 and Fig. 4).

This phenomenon is shown in Figure 4 on a very simple shape : from the 3-4 chamfer distance picture, five points are extracted using (1), while only the center is necessary to get the whole initial shape.

1 1 1	3 3 3	3 3	1 1 1
1 1 1	3 6 3	6	1 5 1
1 1 1	3 3 3	3 3	1 1 1
a	b	c	d

Fig. 4. Pseudo local maxima with $d_{3\text{-}4}$: a pattern (a), the 3-4 chamfer distance picture (b), the local maxima, the four "3" values are pseudo local maxima (c), the modified distance transformed picture, only 5 is a local maxima (d).

These pseudo local maxima can be removed defining a transformation process on the distance transform picture[8,9]. It is a look-up table in which 6 are transformed into 5 and 3 are transformed into 1 (see Fig.4). These new weights are associated with the minimum possible values to generate the same shape. Assuming this transformation on the distance transformed picture, the Medial Axis (that is the centers of maximal disks) can be extracted using the formula (1) (see Fig.6.a).

The Medial Axis points are centered inside the shape, as for a binary skeleton, and the transformation is reversible. Unfortunately medial axes are disconnected. Connecting them is a way to organize the medial axis points, and then to perform shape description because each medial axis point codes a basic area in the original shape.

4. CONNECTION METHOD ON THE 3-4 MEDIAL AXIS

Now we start with a 3-4 medial axis, extracted as previously described. Our target is to connect it to get a medial line, so that the original shape can be analysed through this representation.

When the d_4 or d_8 distance is used, the medial axis is composed of connected

components of points sharing the same distance to the background. The connection can be achieved by initializing some discrete connection paths which start from the connected components, and follow the ridges on the distance transformed picture to reach other medial axis points[10,11,12]. Such an approach is also developed on the hexagonal grid[13].

Using a chamfer distance, the notion of level curves is not that clear, and we would rather speak about level intervals. These intervals are given by [i.m(1,0).. (i+1).m(1,0) -1] and they provide curves which might be both 4- and 8-connected. Then the medial axis is not as clearly disconnected as it was with the City Block or Chessboard distance (see Fig.6.a).

To connect the medial axis, some authors proposed a ridge extraction process, but the result is then very thick, not always connected and needs a final thinning stage[14]. To solve the connection stage with the same kind of algorithm that for simpler distances (we don't want to use an iterative parallel thinning combined with the extraction of medial axis points), we process in two stages :

- *ridge following* : first we follow ridges on the distance picture from the medial axis points, whenever it is possible ;

- *forced propagation* : but some of these paths will end without achieving a connection, and we oblige them to continue until they reach other medial axis or connection points.

Ridge following

This process is initialized scanning the medial axis picture : for each medial axis point A, the ridge following process is recursively called to find medial axis candidates P, which defines the connection paths of the medial line.

Looking at a point P and at its 8-neighborhood on the distance transformed picture (noted DT), we note E = { q in V_8(P) : DT(q) ≥ DT(P) } and we count the number n of 4-connected components in E (this is related to the crossing-number).

If n>0, then inside each component, we look for the points q already labeled as being a medial line point. For the detected points q :

- if DT(P) < DT(q) then we remove the entire component from E (it was already used to build another connection path),

- else we remove only the point q (to avoid multiple connections, but to make sure that we keep at least one).

Now there will exist a propagation from P if the remaining set E is non empty. We keep inside the set E the points which are *ridge candidates*.

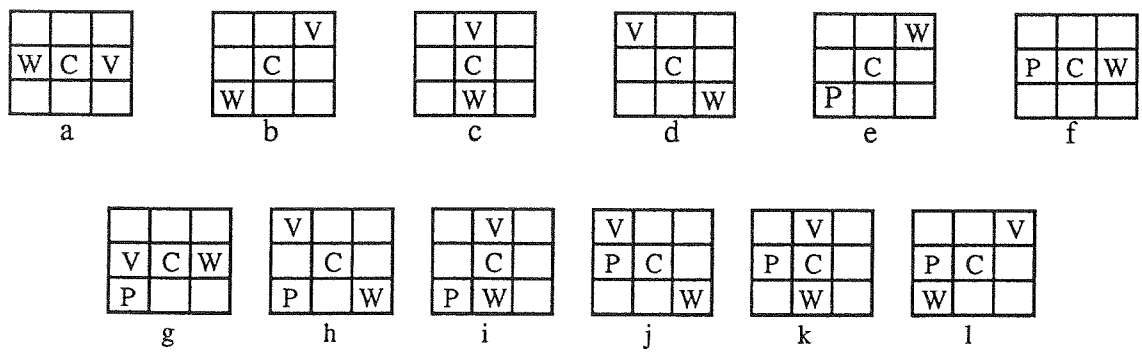

Fig. 5. Detection of ridge points and candidate points.

A point C is a ridge point if there exist V and W such that DT(V) ≤ DT(C) and DT(W) ≤ DT(C), with C,V and W respecting one of the configurations of Fig.5.a-d. A point might be a ridge point for 2 directions.

We say that C is *candidate* if DT(C) ≥ DT(P) and if C is a ridge point in one of the configurations of Figure 5. g-l between P, C, V and W. The configurations of Figure 5.e-f are forbidden.

So given the point P we keep in the set E the points which are also ridge points.

At the end of this test, the set E might be empty. If this situation occurs, there is no more ridge, but we want to achieve the connection, thus we label the point P for a further treatment, called *forced propagation.*

If E is non empty, we keep only one point for each 4-component of E, in order to avoid thick connection ; we choose direct neighbors rather than diagonal neighbors. And the ridge following process is recursively called. It ends when it reachs a point already preserved (medial axis or connection point).

Forced propagations

When, from a point P, no candidate is found, the propagation has to be forced to preserve the connectivity of the medial line. When this situation occurs, there is no ridge to follow, but we can follow the steepest slope (towards higher distance values) and shortest path on the distance transformed picture until we reach a medial axis point.

The resulting medial line is then extracted (see Fig. 6.b).

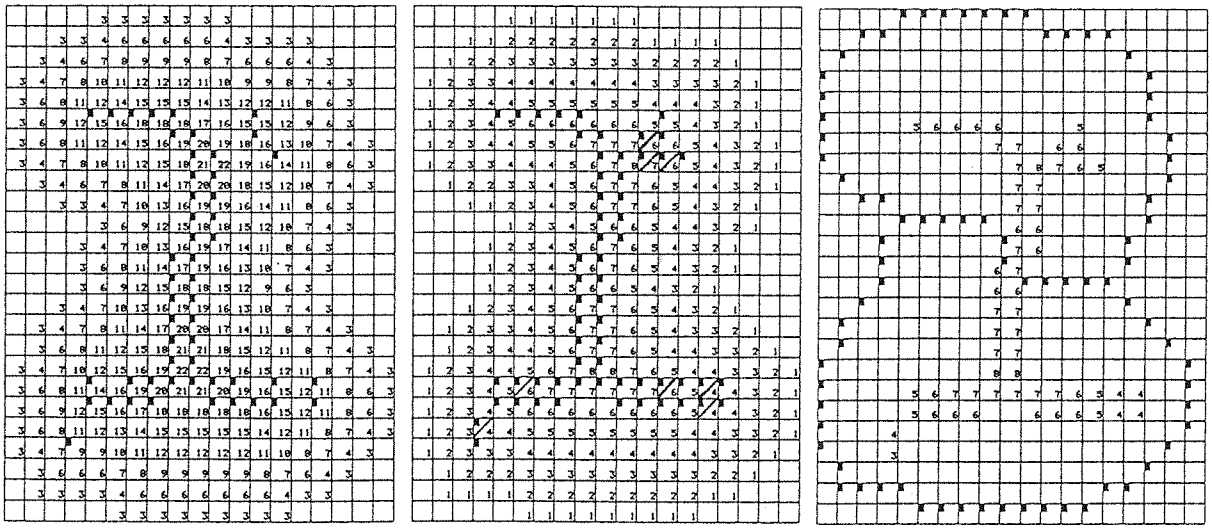

a b c

Fig. 6. Medial axis points are dotted on the distance transformed picture (a), the connection points added to get the medial line are dotted and crossed on the level interval picture (b) and the splitting arcs are drawn (c).

5. SPLITTING PROCESS FROM THE 3-4 MEDIAL LINE

At this stage, we have a medial line which is composed of the medial axis points (so the transformation is reversible) and of connection points. Each point is labeled by its 3-4 distance to the background, thus the medial line represents a covering of the shape by maximal disks, that is elementary areas which are organized together depending on the added connection paths.

To perform shape description with such a structure, the medial line has to be traversed and the weights simultaneously analysed, then the shape manipulation can be processed. For the City Block or the Chessboard distance, this analysis might be performed on the medial line picture itself[15], or a graph representation can be built[12].

The first approach processes completely on the picture (matrix) structure, but the traversal of the medial line has to be performed and adapted each time a new manipulation is expected.

The second approach builds a symbolic representation of the original shape, and as the transformation is reversible, all the manipulations can be performed on this structure and are usually simple because they are some graph analysis methods. Different kinds of shape filtering and shape decomposition methods can be easely developed[16]. For example, to perform a shape splitting we have to find "neck nodes" on a graph structure that is a node such that all its neighbors have a larger weight.

Minima extraction

Using the 3-4 chamfer distance, the nodes of a graph structure should be defined again and in the aim of performing shape splitting, we decided to work only on the medial line picture : local mimima on the medial line are associated with narrowing areas in the shape. The medial line might be locally complicated, which might induce some traversal problems.

These problems are solved using the following process :

- the distance values are divided by three to provide the level intervals on the medial line picture,
- the local minima are extracted processing a traversal of the medial line, if we check the number of connected components with higher weight on the medial line in the 8-neighborhood of the component, this number must be larger than one.

In Figure 6.c, the neck component of the medial line has a weight equal to 7.

Splitting arcs

Now that the components of local minima are detected on the medial line, it remains to draw the splitting arcs. They are drawn following the steepest slope and the shortest path going down on the distance transformed picture (towards smallest values). To initialize them, first we memorize, scanning all the points of the local minima component on the level interval picture, all the directions of steepest slopes. Then we keep one initialization point for each direction ; this point is chosen as close as possible from the centroid of the component.

We show in Figure 6.c the splitting arcs which are generated.

6. RESULTS

Some basic results are presented in Figure 7.a-d, on which the splitting is perfectly performed. We also test the validity of the process on a same shape, but under different orientations (Fig. 7.g). This shape is well decomposed whatever the orientation, while the process using the chessboard distance fails (Fig. 7.h).

Another application concerns material studies (IMG*), for which "cellular concrete" have some aggregations which also need to be separated in order to build a physical model of the material (to study its resistance against some constraints or to simulate heal propagation). The results computed on such a picture are shown in Figure 7.e-f.

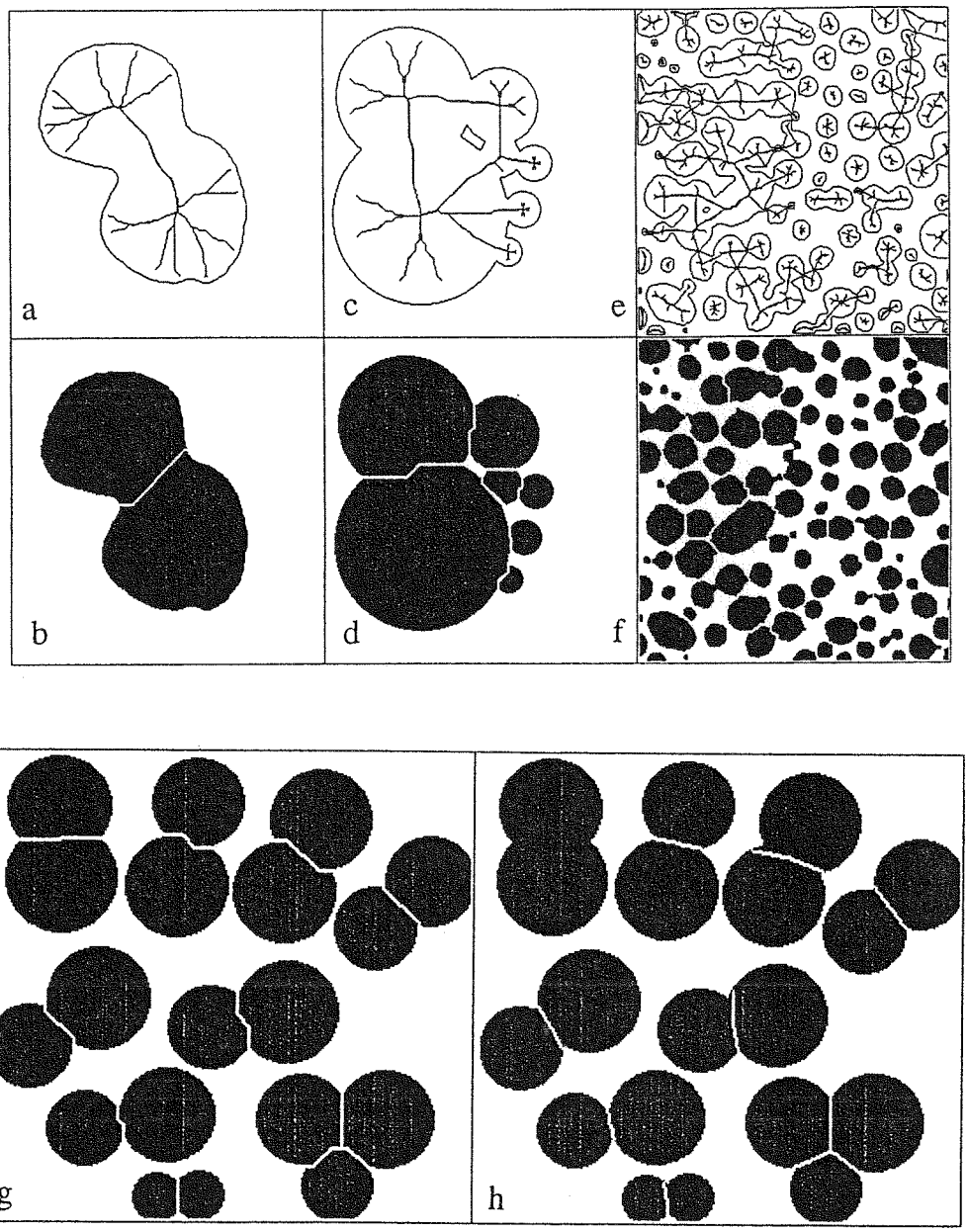

Fig. 7. Results : (a)(c) a shape and its 3-4 medial line, (b)(d) the associated decomposition ; (e) an example of "cellular concrete" with its 3-4 medial line, (f) the separation of seeds which is performed, (g) the decompositions of objects under different orientations performed with their 3-4 medial lines, (h) on the same picture, using the decomposition process with the Chessboard distance : some separations fail.

7. CONCLUSION

We presented a method to perform shape splitting based on medial line representations. A medial line deduced from a 3-4 chamfer distance and its 3-4 medial axis is built and then traversed to extract narrowing points from which splitting arcs are drawn. Because the 3-4 chamfer distance is closer to the euclidean distance than the city block or chessboard distance, the process provides a good invariance under rotations ; it was one of our main targets.

We point out that the process we developed for the 3-4 chamfer distance could be adapted to another chamfer distance and its medial axis without too many important modifications, if the true medial axis is extracted. For these distances, the size of the generating kernel is larger ; the disks are polygons which angles are on some straight lines starting from the central point. These disks become more and more close to the euclidean disks.

We developed the process using a picture approach, but in the aim of performing several kinds of shape manipulations, building a symbolic graph representation is also interesting, because most of the tools developed for the chessboard distance will not need any modification. Such a graph was built for a second aspect of the application we presented in 6.

Finally we mention that the internal decomposition can be completed by analysing the medial line of the background. In the case of material studies, we use this information to complete the internal description and to get a 3D model of the structures.

* This study was supported by the Institut de Mécanique de Grenoble, in collaboration with Jean-Paul Laurent.

REFERENCES

1. J.Serra, "Image Analysis and Mathematical Morphology", Academic Press, London (1989).

2. A.Montanvert and D.Adelh, Tools for shape complexity evaluation and associated decomposition processes, 5th ICIAP, September 1989, Positano (Italy), Published in Progress in Image Analysis and Processing : 348-355 (1990).

3. A.Rosenfeld and J.L.Pfaltz, Distance functions on digital pictures, Pattern Recognition 1: 33-61 (1968).

4. P.E.Danielsson, Euclidean distance mapping, CGIP 14 : 227-248 (1980).

5. I.Ragnemalm, The Euclidean distance transform and its implementation on SIMD architectures, 6th Scand.Conf.on Image Anal., Oulu (Finland) : 379-384 (1989).

6. G.Borgefors, Distance transformations in digital images, CVGIP 34 : 344-371 (1986).

7. A.Rosenfeld and A.C. Kak, "Digital image processing", Academic Press, New-York (1982).

8. C.Arcelli and G.Sanniti di Baja, Weighted distance transforms : a characterization, in proc. of 4th Int. Conf. on IAPR, Cefalu (Italy) : 205-212 (1987).

9. C.Arcelli and G.Sanniti di Baja, Finding local maxima in a pseudo-euclidean distance transform, CVGIP 43 : 361-367 (1989).

10. C.Arcelli and G.Sanniti di Baja, A width-independent fast thinning algorithm, I.E.E.E. trans. on PAMI 7 (4) : 463-474 (1985).

11. C.Arcelli and G.Sanniti di Baja, A one-pass two-operation process to detect the skeletal pixels on the 4-distance transform, IEEE trans. on PAMI 11(4) : 411-414 (1989).

12. A.Montanvert, Median line : graph representation and shape description, in proc. of 8th ICPR. Paris : 430-432 (1986).

13. F. Meyer, Skeletons and perceptual graphs, Signal Processing 16 : 335-363 (1989).

14. F.Y.Shih and C.C.Pu, Medial axis transformation with single-pixel and connectivity preservation using euclidean distance computation, in proc. of 10th ICPR, Atlantic City : 723-725 (1990).

15. C.Arcelli and G. Sanniti di Baja, An approach to figure decomposition using width information, CVGIP 26 : 61-72 (1984).

16. A.Montanvert, Graph environment from medial axis for shape manipulation, in proc. of 4th Int. Conf. on IAPR, Cefalu(Italy) : 197-204 (1987).